Journal of Nuclear Materials 466 (2015) 583–587

Contents lists available at ScienceDirect

Journal of Nuclear Materials

journal homepage: www.elsevier.com/locate/jnucmat

Energetics of gaseous and volatile fission products in molten U–10Zr alloy: A density functional theory study

Ning Wang [a], Jie Tian [a], Tao Jiang [a], Yanqiu Yang [a], Sheng Hu [a], Shuming Peng [a, *], Liuming Yan [b]

[a] Institute of Nuclear Physics and Chemistry, China Academy of Engineering Physics, Mianyang 621999, PR China
[b] Department of Chemistry, Shanghai University, 99 Shangda Road, Shanghai 200444, PR China

ARTICLE INFO

Article history:
Received 1 June 2015
Received in revised form
28 July 2015
Accepted 26 August 2015
Available online 5 September 2015

Keywords:
U-10Zr
Fission products
DFT
Free energy

ABSTRACT

Gaseous and volatile fission products have a number of adverse effects on the safety and efficiency of the U–10Zr alloy fuel. The theoretical calculations were applied to investigate the energetics related to the formation, nucleation, and degassing of gaseous and volatile fission products (Kr, Xe and I) in molten U–10Zr alloy. The molecular dynamics (MD) simulations were applied to generate equilibrium configurations. The density functional theory (DFT) calculations were used to build atomistic models including molten U–10Zr alloy as well as its fission products substituted systems. The vacancy formation in liquid U–10Zr alloy were studied using DFT calculations, with average Gibbs free formation energies at 8.266 and 6.333 eV for U- and Zr-vacancies, respectively. And the interaction energies were −1.911 eV, −2.390 eV, and −1.826 eV for the I–I, Xe–Xe, and Kr–Kr interaction in lattice when two of the adjacent uranium atoms were substituted by gaseous atoms. So it could be concluded that the interaction between I, Kr, and Xe in lattice is powerful than the interaction between these two atoms and the other lattice atoms in U–10Zr.

1. Introduction

Uranium based binary alloys are very promising candidates for core materials in Gen IV nuclear reactors [1,2]. Among these materials, U–Zr alloys have been focused for their simple fabrication procedure as well as good mechanical, thermal and corrosion resistance properties [3,4]. For example, U–Zr alloys have been considered as a nuclear fuel for the SFR [5]. Also, the using of metallic fuel in fast reactor will greatly increase the possibility of closing the nuclear fuel cycle. So they have been studied in several countries such as Japan, China, USA, and Korea.

However, a number of fission gases, xenon (Xe) and krypton (Kr), and volatile fission product iodine (I), are produced and thus bubbles are formed in the fuels as the nuclear burn progresses. The growth of bubbles can result in appreciable fuel swelling, which has a number of adverse effects on the thermo-mechanic properties of the fuel and cladding [6]. Thus the safety and efficiency of the metallic nuclear fuels are affected. In order to get rid of the gaseous and volatile fission products, fuel refabricating is of importance to the recycling of metallic nuclear fuels. Heating up is a promising way to vent the gaseous and volatile fission products from the metallic fuel because of the lower melt point and the higher diffusivity of fission gas atoms in the metallic fuel comparing with those in ceramic fuels [7]. Thermal treating has been used to study the release behaviors of gaseous and volatile fission products from ceramic UO_2 fuel by Hiernaut et al. [8]. For metallic fuel, many models for fission gas release and swelling behavior have been developed [9], but the release behaviors of gaseous and volatile products in high temperature are scarcely reported.

In this study, the theoretical calculations were applied to investigate the energetics related to the formation, nucleation, and degassing of gaseous and volatile fission products (Kr, Xe and I) in molten U–10Zr alloy. The MD simulations were applied to generate equilibrium configurations. The DFT calculations were used to build atomistic models including molten U–10Zr alloy as well as its fission products substituted systems. The free energies of substituted system were also calculated by DFT.

* Corresponding author.
E-mail address: pengshuming@caep.cn (S. Peng).

http://dx.doi.org/10.1016/j.jnucmat.2015.08.050
0022-3115/

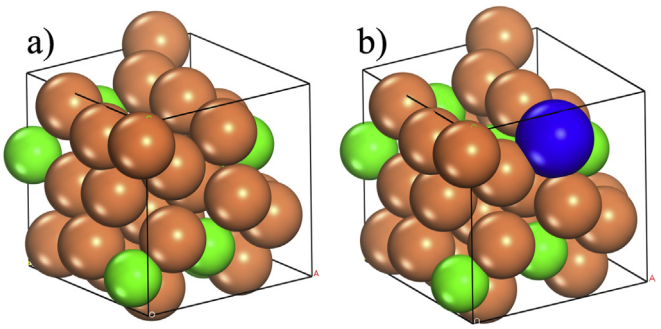

Fig. 1. Schematic diagram of (a) the $U_{26}Zr_{10}$ system, (b) the U-vacancy in the $U_{25}Zr_{10}$ (color code: ochre for U, green for Zr, and blue for U-vacancy). (For interpretation of the references to color in this figure legend, the reader is referred to the web version of this article.)

2. Methodology

2.1. MD simulations and DFT calculations

Both MD simulations and DFT calculations were employed in this study. The MD simulations were carried out using the LAMMPS program [10,11]. And the force field model was developed by fitting the DFT energies and forces of model systems to the EAM by use of the potfit program [12,13]. For details about the force field model and its applications to the study of the molten U–10Zr alloy, the readers are referred to our previous work [14] All the MD simulations were carried out in the NPT ensemble with periodic boundary condition applied at 1 atm pressure and 2000 K corresponding to the molten state of U–10Zr alloy. And the MD simulations are used to generate the equilibrium configurations used for the following DFT calculations.

The DFT calculations were carried out by use of the Vienna Ab-initio Simulation Package (VASP). The initial atomistic models of molten U–10Zr alloy consisted of 26 U atoms and 10 Zr atoms corresponding approximately to the composition of U–10Zr alloy. By removal of one or two U atoms (Zr atoms) from the initial atomistic models, atomistic models with one or two U-vacancies (Zr-vacancies) were created. If one or two of the U atoms were substituted by X atoms, atomistic models with fission products were obtained. Though these atomistic models did not correspond exactly to the real world metallic nuclear fuels as the concentrations of fission products were much lower in real world, these atomistic models would not significantly deviate from these atomistic models as long as the substituted atoms were separated in lattice. In all the DFT calculations, periodic boundary conditions were applied to the atomistic models. The PBE functional with supplement of a Hubbard *U* was applied to calculate the energetics using plane wave basis set and pseudo-potentials as implemented in the VASP program [15–19]. And a Hubbard *U* at 1.24 eV was used for both uranium and zirconium atoms [14]. We noticed the very different arguments about the choices of Hubbard *U* values for metals. For example, Xie et al. concluded that Hubbard values of 1.24 and 0.0 eV for U and Zr provide the best statistical agreement with experiments [20], however, Söderlind et al. argued that this assertion by Xie et al. is incorrect [21]. Söderlind et al. further argued that the choice by Xie et al. predicts negative enthalpy of mixing in the U–Zr alloy system contradicting conventional DFT as well as one of the main features of the experimental U–Zr phase diagram. In our previous work, we developed an EAM for the U–10Zr alloy based on DFT calculations by use of the same Hubbard *U* value of 1.24 eV for both uranium and zirconium atoms and predicted positive mixing enthalpy at 48.8 mV [14]. Though our predicted mixing enthalpy is still smaller than the experimental value at about 80 mV, it is much closer than the mixing enthalpy predicted by Xie et al., therefore, it is convincible to use the same Hubbard *U* of 1.24 eV for both uranium and zirconium atoms [22]. The electronic wave functions, with spin-polarization allowed, were expanded using the plane wave basis functions with cutoff energy of 600 eV and digitized using the tetrahedron algorithm with Blöchl corrections [23]. The Brillouin-zone integrations were carried out using the Monkhorst-Pack grids with a $4 \times 4 \times 4$ mesh for all the atomistic models [24], and the convergent criterion for total energy was set to 0.001 eV for all the calculations.

2.2. Energetics of bubble nucleation in molten U–10Zr alloy

The energetics of fission products, including Kr, Xe, and I, in the molten U–10Zr alloy were calculated as follows: Firstly, MD simulations were carried out for the molten U–10Zr alloy, and equilibrium configurations were obtained. And then, DFT calculations were conducted for these configurations with periodic boundary conditions applied, and overall Gibbs free energies as well as entropies were obtained. Finally, one or two of the uranium atoms were substituted by a fission product, and the overall Gibbs free energies of the substituted systems were obtained. Finally, the various Gibbs free energies were obtained.

3. Results and discussion

3.1. Vacancy formation energies

3.1.1. Gibbs free formation energy of U-vacancy

In Fig. 1, it showed the schematic diagram of a $U_{26}Zr_{10}$ system and a U-vacancy in the $U_{25}Zr_{10}$ system. The U-vacancy was formed by removal of a U-atom from the $U_{26}Zr_{10}$ system,

$$U_{26}Zr_{10} \rightarrow U_{25}Zr_{10} + U \quad (1)$$

and the Gibbs free formation energy of U-vacancy was evaluated as,

$$\Delta G_f(U_{vac}) = \Delta G_f(U_{25}Zr_{10}) + \Delta G_f(U) - \Delta G_f(U_{26}Zr_{10}) \quad (2)$$

where $\Delta G_f(U_{26}Zr_{10})$ and $\Delta G_f(U_{25}Zr_{10})$ are total Gibbs free energies of the $U_{26}Zr_{10}$ and the $U_{25}Zr_{10}$ systems, and $\Delta G_f(U)$ is Gibbs free energy or chemical potential of a U atom evaluated from liquid uranium using the same DFT method [25]. However, the Gibbs free formation energy of U-vacancy depends on which U-atom was removed or the location of the U-vacancy. In order to evaluate the average Gibbs free formation energy of U-vacancy, one of the U-atoms was removed from all possible locations at each time, and

Table 1
Gibbs free formation energies of vacancies and of X-substitutions in the molten U–10Zr alloy (units, eV).

Systems	Gibbs free energy	ΔE
U	−3.902	0.000
Zr	−2.154	0.000
Kr	−0.030	0.000
Xe	−0.005	0.000
I	−0.324	0.000
$U_{26}Zr_{10}$	−359.147	0.000
$U_{25}Zr_{10}$	−346.978	8.266
$U_{26}Zr_9$	−350.660	6.333
$U_{25}Zr_{10}Kr$	−341.968	13.306
$U_{25}Zr_{10}Xe$	−340.412	14.837
$U_{25}Zr_{10}I$	−346.898	8.671
$U_{24}Zr_{10}Kr_2$	−326.615	24.786
$U_{24}Zr_{10}Xe_2$	−324.067	27.286
$U_{24}Zr_{10}I_2$	−336.559	15.431